The position of the double bond in monounsaturated free fatty acids is essential for the inhibition of the nicotinic acetylcholine receptor

ARTICLE *in* BIOCHIMICA ET BIOPHYSICA ACTA · JUNE 2012

Impact Factor: 4.66 · DOI: 10.1016/j.bbamem.2012.06.001 · Source: PubMed

5 AUTHORS, INCLUDING:

Vanesa Liliana Perillo
University of Vermont
9 PUBLICATIONS **5** CITATIONS
SEE PROFILE

Ana S Vallés
Centro Cientifico-Tecnologico Bahia Blanca
12 PUBLICATIONS **188** CITATIONS
SEE PROFILE

Francisco J Barrantes
Pontifical Catholic University of Argentina
220 PUBLICATIONS **4,427** CITATIONS
SEE PROFILE

Biochimica et Biophysica Acta 1818 (2012) 2511–2520

Contents lists available at SciVerse ScienceDirect

Biochimica et Biophysica Acta

journal homepage: www.elsevier.com/locate/bbamem

The position of the double bond in monounsaturated free fatty acids is essential for the inhibition of the nicotinic acetylcholine receptor

Vanesa L. Perillo [a], Gaspar A. Fernández-Nievas [a,1], Ana S. Vallés [a], Francisco J. Barrantes [b], Silvia S. Antollini [a,*]

[a] Instituto de Investigaciones Bioquímicas de Bahía Blanca, Consejo de Investigaciones Científicas y Técnicas (CONICET)/Universidad Nacional del Sur, Camino La Carrindanga km. 7, B8000FWB Bahía Blanca, Argentina
[b] Laboratory of Molecular Neurobiology, Biomedical Res. Progr. UCA-CONICET, Av. A. Moreau de Justo 1600, 1107 Buenos Aires, Argentina

ARTICLE INFO

Article history:
Received 30 March 2012
Received in revised form 31 May 2012
Accepted 4 June 2012
Available online 12 June 2012

Keywords:
Nicotinic acetylcholine receptor
Lipid–protein interaction
Free fatty acid
Fluorescence spectroscopy
Electrophysiology

ABSTRACT

Free fatty acids (FFAs) are non-competitive antagonists of the nicotinic acetylcholine receptor (AChR). Their site of action is supposedly located at the lipid-AChR interface. To elucidate the mechanism involved in this antagonism, we studied the effect that FFAs with a single double-bond at different positions (ω6, ω9, ω11 and ω13 *cis*-18:1) have on different AChR properties. Electrophysiological studies showed that only two FFAs (ω6 and ω9) reduced the duration of the channel open-state. The briefest component of the closed-time distribution remained unaltered, suggesting that ω6 and ω9 behave as allosteric blockers. Fluorescence resonance energy transfer studies indicated that all FFAs locate at the lipid-AChR interface, ω6 being restricted to annular sites and all others occupying non-annular sites. The perturbation of the native membrane order by FFAs was evaluated by DPH (1,6-diphenyl-1,3,5-hexatriene) and Laurdan fluorescence polarization studies, with the greatest decrease observed for ω9 and ω11. AChR conformational changes produced by FFAs present at the lipid bilayer were evaluated by fluorescence quenching studies of pyrene-labeled AChR and also using the AChR conformational-sensitive probe crystal violet. All *cis*-FFAs produced AChR conformational changes at the transmembrane level, but only ω9, ω11 and ω13 perturbed the resting state. Thus, the position and isomerism of the torsion angle of unsaturated FFAs are probably a key factor in terms of AChR blockage, suggesting that FFAs with a unique *cis* double bond at a superficial position inside the membrane directly inhibit AChR function by perturbing a potential conserved core structure for AChR gating at that level.

1. Introduction

The nicotinic acetylcholine receptor (AChR) is an integral membrane protein embedded in the postsynaptic membrane and composed of five homologous subunits organized around a central pore [1]. All subunits consist of an amino-terminal extracellular domain followed by four transmembrane (TM) hydrophobic domains 20–30 amino acids long (M1 through M4) connected to one another by loops of varying length, and ending with a very short extracellular carboxyl terminus [2]. The AChR TM domain is arranged in three concentric rings: the M2 TM segments of each subunit form the inner ring, constituting the ion channel itself; the M1 and M3 TM-segments make up the middle ring, and the M4 TM-segments form the outer ring, which is the TM-segment closest to the lipid microenvironment [3,4]. ESR studies have identified differences between the signals proceeding from bulk membrane lipids and those from the protein-immobilized lipid that surrounds the AChR in native and reconstituted membranes [5,6]. Thus, it is possible to distinguish an annular lipid layer surrounding the AChR [5] and non-annular lipids inserted between the different TM domains of the protein. These two types of lipid environments have distinct compositions and hence different biophysical properties [7].

The AChR is an allosteric protein, switching between open and closed states. Ligand binding regulates the conformational paths of AChR opening and desensitization, possibly through several intermediate states [8]. The AChR has two closed stable functional states – the resting state (R) in the absence of agonist and the slow-onset desensitized state (D) in the presence of agonist– and two metastable functional states: a fast-onset desensitized state and an open state [9,10]. Previous studies using reconstituted membranes have found that the proportion of receptors in the R and D states appears to depend on the final lipid composition, regardless of the presence or absence of agonist [11], leading to the conclusion that modulation of

Abbreviations: ACh, acetylcholine; AChR, nicotinic acetylcholine receptor; Carb, carbamylcholine; Chol, cholesterol; CrV, crystal violet; DPH, 1,6-diphenyl-1,3,5-hexatriene; FFAs, free fatty acids; sFFAS, saturated free fatty acids; *cis*-FFAs, *cis*-unsaturated free fatty acids; *trans*-FFAs, *trans*-unsaturated free fatty acids; GP, generalized polarization; NCA, non-competitive antagonists; N-PyrM, N-(1-pyrenyl)maleimide; POPA, palmitoyl-oleoyl phosphatidic acid; POPC, palmitoyl-oleoyl phosphatidylcholine; 5-SLFA, 5-spin labeled fatty acid; TM, transmembrane; FRET, Förster-type resonance energy transfer

* Corresponding author at: Instituto de Investigaciones Bioquímicas de Bahía Blanca, B8000FWB Bahía Blanca, Argentina. Tel.: +54 291 486 1201; fax: +54 291 4861200.
E-mail address: silviant@criba.edu.ar (S.S. Antollini).
[1] In memory (deceased 2009).

0005-2736/$ – see front matter © 2012 Elsevier B.V. All rights reserved.
doi:10.1016/j.bbamem.2012.06.001

the AChR is lipid-dependent. Furthermore, lipid-inactivated AChR is in neither the R nor the D state, but adopts a novel conformation whereby the allosteric coupling between the neurotransmitter-binding sites and the TM pore is lost. Previous studies from our laboratory and other authors have suggested that the M4 TM helix acts as a lipid-sensor, linking bilayer properties to AChR function [12–14].

Free fatty acids (FFAs) have been found to inhibit the AChR in a noncompetitive manner [4,8–15]. Minota and Watanabe suggested that this inhibition by FFAs may occur through their action on allosteric sites of the AChR [16]. Among all lipids tested, FFAs were the ones with the highest affinity for the native membrane-bound AChR, at the AChR-lipid interface [7,17]. One of the preferred targets of FFAs appears to be the non-annular boundary lipid-AChR domain [13,18,19], although FFAs also bind to other classes of sites. Recently, we demonstrated that FFAs modulate AChR function by a mechanism of action different from that used by other hydrophobic inhibitors of the AChR, such as steroids [14]. The direct contact between exogenous FFAs and the AChR TM segments might remove the AChR from its R state, causing its functional inhibition. We also postulated a possible relationship between the membrane physical state and the AChR conformational state, which would explain why the AChR activation equilibrium is affected by changes in the lipid microenvironment [14].

In the present work we focused our attention on the effect of *cis*-monounsaturated FFAs with the double bond at different positions along the hydrocarbon chain on AChR function, also looking at the protein–lipid interface in native *Torpedo californica* membranes. Functionality was studied using the patch-clamp technique in the cell-attached configuration in the presence or absence of FFAs. In an attempt to understand the effect of these FFAs on the modulation of AChR conformation, we used the fluorescent dye crystal violet (CrV), which has higher affinity for the D state than for the R state of AChR, and quenching experiments of a pyrene-labeled AChR reconstituted in a model system. Membrane order perturbations by FFA addition were followed with the fluorescence probes DPH and Laurdan. Laurdan molecules were also used to study FFA location at both annular and non-annular sites. Only two *cis*-unsaturated FFAs inhibit and generate conformational changes in the AChR whereas most of the FFAs modified the AChR conformational state and biophysical properties of the membrane. Furthermore, not all FFAs locate at the same sites at the lipid-AChR interface.

2. Materials and methods

2.1. Materials

T. californica specimens obtained from the Pacific coast of California (Aquatic Research Consulants, San Pedro, CA) were killed by pithing, and the electric organs were dissected and stored at −70 °C until use. Laurdan and pyrene-maleimides were purchased from Molecular Probes (Eugene, OR). Affi-Gel® 10 Gel and dithiothreitol were obtained from Bio-Rad. Synthetic lipids and 5-spin labeled fatty acid (5-SLFA) were from Avanti Polar Lipids, Inc. (Birmingham, AL). Crystal violet (CrV) and all other drugs were obtained from Sigma-Aldrich.

2.2. Methods

2.2.1. Preparation of AChR-rich membranes

AChR-rich membrane fragments were prepared from *T. californica* electric tissue as described previously [20]. Briefly, electric tissue was chopped into small pieces, homogenized using a Virtis homogenizer under controlled conditions, and submitted to a series of centrifugation steps ending in a high-speed sucrose gradient centrifugation. The obtained middle fraction corresponds to AChR-rich membranes with a specific activity of the order of 1.0–1.5 nmol of α-bungarotoxin sites/mg of protein [20]. The orientation of AChR in the membrane vesicles was determined by comparing the toxin binding sites in the presence and in the absence of Triton X-100 as described by Hartig and Raftery [21,22].

2.2.2. Affinity column preparation and AChR purification

T. californica crude membranes were solubilized in 1% sodium cholate (2 mg/ml protein concentration) for 45 min at 4 °C and then centrifuged at 74,000×g for 1 h to discard the insoluble material. The AChR was purified by affinity chromatography in the presence of synthetic lipids [23,24]. Briefly, the affinity column was prepared by coupling cystamine to Affi-Gel 10, reduction with dithiothreitol, and final modification with bromoacetylcholine bromide. The supernatant was applied to the affinity column. To facilitate complete exchange of endogenous for defined lipids, the column was then washed with a linear gradient of defined lipids (POPC:POPA:Chol 3:1:1) dissolved in dialysis buffer (100 mM NaCl, 0.1 mM phosphate, 0.1 mM EDTA, 0.02% NaN_3, pH 7.8) containing 1% cholate, from 1.3 to 3.2 mM and then to 0.13 mM lipid concentration [23]. The AChR was then eluted from the column with a 0.13 mM lipid solution in 250 mM NaCl, 0.1 mM EDTA, 0.02% NaN_3, 5 mM phosphate, pH 7.8, with 0.5% cholate and 10 mM carbamylcholine (Carb). After elution from the column, the AChR was dialyzed against 1 l of dialysis buffer with five buffer changes (every 12 h) at 4 °C. AChR purity was checked by SDS-PAGE, and protein concentration was determined by the method of Lowry [25]. The samples were stored at −70 °C until use.

2.2.3. N-(1-pyrenyl)maleimide AChR labeling

The labeling of TM AChR cysteines was performed according to Li et al. [26] and Narayanaswami et al. [27,28] with slight modifications as described in Fernández Nievas *et al.* [14]. Briefly, purified AChR solubilized in 1% cholate (1 mg/ml) was incubated in the presence of 1 mM N-PyrM for 1 h at room temperature with gentle shaking. The solution was centrifuged at 70,000×g for 45 min to pellet aggregates. The supernatant was dialyzed against 1 l of dialysis buffer with five buffer changes (every 12 h) at 4 °C and stored at −20 °C until use. N-PyrM-AChR samples were submitted to SDS-PAGE, and the N-PyrM label was visualized under a UV transilluminator showing that the band corresponding to the γ subunit was predominantly labeled.

2.2.4. Preparation of free fatty acid solutions and titration of membrane fragments

Petroselenic acid (*cis*-18:1ω-6), oleic acid (*cis*-18:1ω-9), vaccenic acid (*cis*-18:1ω-11), *cis*-13-octadecenoic acid (*cis*-18:1ω-13) and elaidic acid (*trans*-18:1ω-9) were dissolved in ethanol. After each FFA addition, samples were kept at 25 °C for 45 min to allow equilibration of the FFA with the membrane. In all cases the amount of ethanol added to the samples was kept below 0.5%.

2.2.5. Cell culture

CHO-K1/A5 cells stably expressing adult muscle AChR [29] were cultured in Ham F12 medium supplemented with 10% bovine fetal serum and 40 mg/ml of the selection antibiotic G418 (Sigma) in the cell medium.

2.2.6. Single-channel recordings

Single-channel currents were recorded in the cell-attached configuration [30] at a membrane potential of −70 mV and 20 °C using an Axopatch 200B patch-clamp amplifier (Axon Instruments, Inc., Foster City, CA), digitized at 94 kHz with an ITC-16 interface (Instrutech Corporation, Long Island, New York, NY) and transferred to a computer using the program Acquire (Bruxton Corporation, Seattle, WA). The bath and pipette solutions contained 142 mM KCl, 5.4 mM NaCl, 1.8 mM $CaCl_2$, 1.7 mM $MgCl_2$ and 10 mM N-2-hydroxyl piperazine-N0-2-ethane sulfonic acid, pH 7.4. Patch pipettes were pulled from Kimax-51 capillary tubes (Kimble Products, Vineland, New Jersey, USA), coated with Coat D (M-Line accessories, Measurements Group, Raleigh, NC) and fire-polished. Pipette resistances ranged from 5 to

7 MΩ. ACh at a final concentration of 1 μM was present in the pipette solution. FFAs (*cis*-18:1ω-6; *cis*-18:1ω-9; *trans*-18:1ω-9; *cis*-18:1ω-11 and *cis*-18:1ω-13) were prepared from a 20 mM stock solution and stored at −20°C. The FFA was dissolved in the cell medium (60 μM) for 30 min at 37 °C prior to each experiment to allow equilibration of the FFA with the cell membrane. Medium was then replaced with bath solution and 1 μM ACh was applied to the cell from the pipette tip. Detection of single-channel events using the program TAC (Bruxton Corp.) followed the half-amplitude threshold criterion at a bandwidth of 5 kHz. Open, burst and closed-time histograms were plotted using a logarithmic abscissa and square-root ordinate and fitted to the sum of exponential functions by the maximum likelihood criterion using the program TACFit (Bruxton Corp.). Burst resolution was obtained from the delay between the main closed-time component and the succeeding one. Data are expressed as mean ± S.D. from independent experiments. Statistical analysis was performed using Student's *t*-test.

2.2.7. Fluorescence measurements

AChR-rich membranes and N-PyrM-AChR were suspended in buffer A (150 mM NaCl, 0.25 mM $MgCl_2$, and 20 mM HEPES buffer, pH 7.4) at a final concentration of 50–100 μg of protein/ml (0.2–0.4 μM) or 20 μg/ml, respectively. The optical density of the membrane suspension was kept below 0.1 to minimize light scattering. All fluorimetric measurements were performed in an SLM model 4800 fluorimeter (SLM Instruments, Urbana, IL) using a vertically polarized light beam from Hannovia 200-W mercury/xenon arc obtained with a Glan-Thompson polarizer (4-nm excitation and emission slits) and 2-ml quartz cuvettes. The temperature was set at 25 °C with a thermostated circulating water bath (Haake, Darmstadt, Germany).

2.2.8. Generalized polarization (GP) determination

Laurdan was added to AChR-rich membrane samples (50 μg protein/ml) from an ethanol solution to give a final probe concentration of 0.6 μM. The amount of organic solvent was kept below 0.2%. The samples were incubated for 45 min before the addition of increasing concentrations of the different FFAs. Each addition was followed by a further 45-min incubation to allow equilibration, and then the emission spectra were collected. GP values were obtained from emission spectra using an excitation wavelength of 290 nm or 360 nm, for Förster-type resonance energy transfer (FRET) or direct excitation, respectively, as follows

$$GP = (I_{434} - I_{490})/(I_{434} + I_{490})$$

where I_{434} and I_{490} are the emission intensities at the characteristic wavelength of the gel and liquid-crystalline phases, respectively [31,32].

2.2.9. Anisotropy measurements

AChR-rich membranes (50 μg protein/ml) reconstituted in buffer A were incubated with the fluorescence probe 1,6-diphenyl-1,3,5-hexatriene (DPH) (0.6 μM final concentration) for 45 min, followed by the addition of increasing concentrations of the FFAs. The samples were incubated again for 45 min before anisotropy (*r*) measurements. The excitation and emission wavelengths used were 365 and 425 nm, respectively. Fluorescence anisotropy measurements were done in the T format with Schott KV418 filters in the emission channels and corrected for optical inaccuracies and background signals. The anisotropy value, *r*, was obtained according to the following equation [33]:

$$r = \left((I_v/I_h)_v - (I_v/I_h)_h\right)/\left((I_v/I_h)_v + (I_v/I_h)_h\right)$$

where $(I_v/I_h)_v$ and $(I_v/I_h)_h$ are the ratios of the emitted vertical or horizontally polarized light to the exciting, vertical or horizontally polarized light, respectively. The *r* value can range between −0.2 and 0.4, higher values denoting higher structural lipid order [34].

2.2.10. Förster resonance energy transfer (FRET) measurements

The energy transfer efficiency (*E*) in relation to all other deactivation processes of the excited donor depends on the sixth power of the distance between donor and acceptor. According to Förster's theory [35] *E* can be calculated as follows:

$$E = 1 - (I/I_0)$$

where *I* and I_0 are the emission intensities in the presence and in the absence of the acceptor, respectively. Here, *I* corresponds to the maximal intrinsic protein emission intensity, which is 330 nm. The excitation wavelength was set at 290 nm.

T. californica AChR-rich membranes (50 μg protein/ml) were incubated with the fluorescence probe Laurdan for 45 min. Initial fluorescence measurements were taken before the addition of the Laurdan probe. Increasing concentrations of the FFAs were then added, followed by a 45-min incubation before taking the fluorescence emission spectra. For each condition, the normalized FRET efficiency was calculated as follows:

$$E_{nor} = \left(I - I^{lau}\right)/\left(I_0 - I_0{}^{lau}\right)$$

where I_0^{lau} and I_0 values are the initial emission intensities of the samples with or without Laurdan for any given condition, respectively.

2.2.11. CrV fluorescent measurements

CrV experiments were conducted as described previously [14]. AChR-rich membranes were suspended in buffer A (100 μg of protein/ml) and incubated with FFAs for 45 min. For measurements conducted with the AChR in the desensitized state, *T. californica* membranes were incubated with 0.5 mM Carb for 15 min following the FFA addition. The membranes were subsequently titrated with increasing concentrations of CrV (in buffer A). After each addition of CrV the samples were incubated for 15 min before obtaining the fluorescence emission spectra. CrV was excited at 600 nm, and the fluorescence emission spectra were collected from 605 to 700 nm. Before the first addition of CrV, a background fluorescence emission spectrum was obtained for each sample. The spectrum was then subtracted from the emission spectra obtained in the presence of CrV and the maximum intensity (at 623–625 nm) was measured. To determine the CrV dissociation constants (K_D), the value of the CrV maximum fluorescence emission was plotted as a function of the logarithmic CrV concentration (M). The resulting sigmoid curve was fitted to the Boltzmann function and the K_D was calculated.

2.2.12. Fluorescence quenching with a spin-label FFA

Quenching experiments were done using N-PyrM AChR. The excitation wavelength was 345 nm and the maximum pyrene fluorescence emission was recorded at 373 nm. N-PyrM-AChR samples (20 μg/ml) were incubated with the different FFAs (60 μM). Samples with or without FFA were then titrated with increasing concentrations of 5-SLFA or with vehicle (ethanol) only and incubated for 30 min at 25 °C prior to the fluorescence measurement in order to let the 5-SLFA reach equilibrium with the sample. From the fluorescence data, Stern–Volmer plots were obtained according to the equation:

$$F_0/F = 1 + K_{sv}[Q]$$

where F_0 and *F* correspond to the fluorescence emission of N-PyrM-AChR in the absence and presence of 5-SLFA, respectively, [*Q*] is the concentration of the quencher, and K_{sv} is the Stern–Volmer constant [36], a measure of the quencher concentration in the vicinity of the fluorophore.

3. Results

We used a variety of mono-unsaturated FFAs (*cis*-18:1ω-6, *cis*-18:1ω-9, *cis*-18:1ω-11, *cis*-18:1ω-13, and *trans*-18:1ω-9) to study the possible relationship between the position of the double bond and the perturbation of AChR function, AChR conformation and membrane fluidity. Fig. 1 shows representative chemical structures of the five different FFAs tested. The gradual displacement of the kink with the variation in the position of the single double bond of the FFAs and the wide divergence between the broken chain of the *cis*-unsaturated FFAs and the linear chain of the *trans*-unsaturated FFAs become apparent.

3.1. FFA location at the lipid-AChR interface

To determine whether the different FFAs studied were bound either to annular lipid sites or non-annular lipid sites or both, FRET studies were performed between the intrinsic fluorescence of *Torpedo* AChR as donor and Laurdan probe as acceptor. FRET efficiency between this acceptor–donor pair was introduced by our group [37] and subsequently used to disclose different phospholipid (PC) and cholesterol sites on the AChR surface [19]. It was observed that both types of lipids elicited displacements of the fluorescent probe and that such displacements were not only independent of one another but also additive, and that Laurdan displacement elicited by FFAs alone amounted to the sum of the effects caused by PC and cholesterol together. It was thus possible to distinguish PC sites from cholesterol sites, both of which are accessible to FFAs. Furthermore, considering that PC and cholesterol are typical examples of annular and non-annular lipids, respectively, we argued that a) if Laurdan can sense different types of sites at the lipid–protein interface, Laurdan is expected to be located at these sites; and b) the two different sites shown by Laurdan may correspond to annular and non-annular sites, as originally postulated by Jones and McNamee [18] and Narayanaswami and McNamee [27] following a different methodology (AChR covalently labeled with N-(1-pyrenyl)maleimide and brominated lipids as quenchers). Recent studies from our group showed that the profile of the curves obtained with normalized FRET efficiency (ΔE) values as a function of the concentration of an exogenous hydrophobic molecule is related to their binding to distinct sites at the AChR-lipid interface. This is due to the displacement of acceptor molecules (Laurdan) from the AChR microenvironment by the addition of an exogenous molecule. We therefore proposed that the decrease in E could be dissected into two characteristically different regions [13]. The steep initial slope is a consequence of the higher affinity of exogenous lipids to annular sites which provoke the displacement of Laurdan from them [38]. The second slope, a linear decrease in E, is related to annular sites, implying Laurdan displacement by exogenous lipids which are rapidly exchanged with the rest of the membrane lipids.

Here, AChR-rich membranes previously labeled with Laurdan were titrated with the different FFAs and the fluorescence measurements carried out. As Fig. 2 shows, the presence of most of the *cis*-monounsaturated acids (*cis*-18:1ω-9, *cis*-18:1ω-11 and *cis*-18:1ω-13) inside the membrane caused a significant diminution in the normalized ΔE –more than a 50% decrease with respect to control values. Only *cis*-18:1ω-6 induced a small decrease in ΔE values (less than 15% diminution compared to control values). Comparing the present results with those of previous work [13], we can infer that the profile of diminution of the normalized ΔE, caused by the presence of *cis*-18:1 ω-6 in the membrane is caused by the location of this FFA only in annular sites, whereas the rest of the *cis*-FFAs (*cis*-18:1ω-9, *cis*-18:1ω-11 and *cis*-18:1ω-13) locate both in annular and non-annular sites.

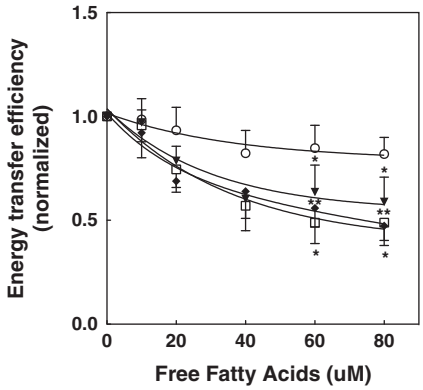

Fig. 2. Changes in normalized FRET efficiency (E) between intrinsic fluorescence in native *T. californica* AChR-rich membrane and Laurdan upon addition of increasing concentrations of *cis*-18:1ω-6 (○), *cis*-18:1ω-9 (□), *cis*-18:1ω-11 (♦) and *cis*-18:1ω-13 (▼). The *E* values obtained in the presence of FFAs were normalized with respect to the corresponding *E* value in its absence (100%). Each point corresponds to the average ± S.D. of more than four independent experiments. Statistically significant differences (*, $p<0.05$ and **, $p<0.01$) compared with the control values.

3.2. Inhibition of the AChR by FFA

Previous results from our laboratory using the patch-clamp technique in the cell-attached configuration demonstrated that *cis*-18:1ω-9 behaves as an AChR inhibitor [39]. Here, similar studies were performed in order to evaluate the effect of other monounsaturated FFAs on AChR single-channel kinetics. Control recordings obtained in the presence of low agonist concentration (1 μM ACh) in the pipette solution showed the characteristic sparse AChR channel openings, occasionally interrupted by brief closures (Fig. 3). The distribution of single-channel openings and burst durations fitted well with a single exponential component in both cases. Table 1 shows the kinetic parameters obtained. In most of the recordings, the distribution of the closed-time duration was described by two components. The longest component was variable and depended on the number of AChR channels in the patch, as described by Sine and Steinbach [40]. The briefest component was minor and as previously reported very likely corresponds to the reopening of the closed channel [40].

When a 30 min pre-incubation with 60 μM *cis*-18:1ω-9 was performed before patch channel recordings with AChR (1 μM) in the pipette, statistically significant differences between the channel open-state duration of control and FFA-exposed channels were found

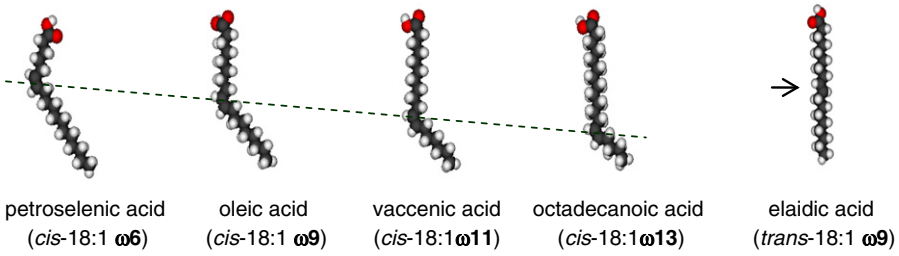

Fig. 1. Molecular structures of the FFAs studied in this work. The break line shows the position of the *cis* double bond and the arrow indicates the position of the *trans* double bond.

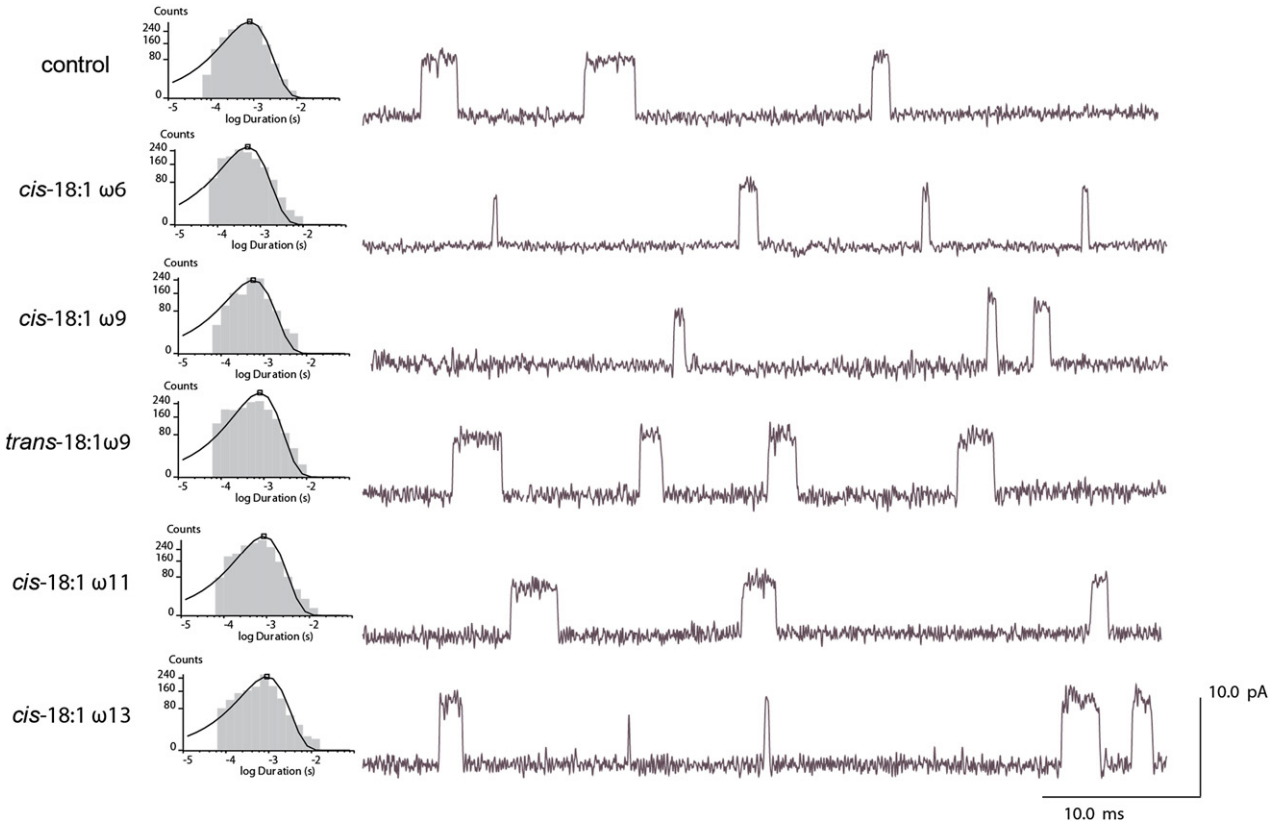

Fig. 3. Single-channel patch-clamp recordings of ACh-activated channels in CHO-K1-A5 cells. Open time histograms (left) resulting from the analysis of the single-channel recordings and raw traces of single-channel currents (right) obtained in the cell-attached configuration from CHO-K1/A5 cells expressing adult AChR activated by ACh (1 μM) in the absence or the presence of the indicated FFA (60 μM). Membrane potential: -70 mV.

(Table 1), confirming previous results [39]. Similar results were obtained in the presence of 60 μM *cis*-18:1ω-6. However, no changes were observed in the channel mean open duration when incubations were performed in the presence of 60 μM of FFAs with the double bond at deeper positions inside the bilayer (*cis*-18:1ω-11 or *cis*-18:1 ω13), or with 60 μM of *trans*-18:1ω-9. Compared to the control condition, closed-time distributions showed no modifications in either the duration or the area of the briefer component of the closed time histogram in the presence of any of the FFAs tested. Furthermore, the channel amplitude was not significantly modified by exposure to FFAs. Burst-time histograms were composed in all cases of one component similar in duration to the open-time component, probably reflecting single apertures. Thus, when cells were pre-incubated with either 60 μM *cis*-18:1ω-9 or *cis*-18:1ω-6, a statistically significant decrease of this component was evidenced in accordance with the diminution of the mean open time, thus confirming AChR current inhibition by these two FFAs.

3.3. Biophysical properties of AChR-rich membranes treated with FFAs

Considering that only two of the five FFAs tested (the ones with the double bond at a more superficial position inside the membrane) modified AChR function, we next studied the biophysical properties of AChR-rich membranes in the presence of different FFAs.

Owing to the effect of dipolar relaxation processes, Laurdan has the physical capacity to sense the molecular dynamics and polarity in its environment [31,32]. The principal dipoles sensed by Laurdan in the membrane are water molecules [41]. The extent of their penetration in the local membrane packing gives a measure of the phospholipid order. GP values calculated from Laurdan spectra therefore provide information on the fluidity of the membrane [41,42]. We found a direct correlation between FFA structure and membrane perturbations. Fig. 4a shows that once incorporated into the membrane, the *trans*-unsaturated FFAs induced a slight and saturable decrease in the GP values, resulting in a curve similar to that of the control,

Table 1
AChR channel properties in the presence of a fixed concentration of FFAs (60 μM). Currents were measured following the patch-clamp technique in the cell-attached configuration from CHO-K1/A5 cells expressing adult AChR. Each data corresponds to the average ± S.D. values.

	Amplitude (pA)	τ_{open} (ms)	τ_{burst} (ms)	τ_{closed} (briefest component)		n
				(ms)	(area)	
Control	5.31 ± 0.64	0.85 ± 0.09	0.99 ± 0.14	0.14 ± 0.07	0.051 ± 0.016	10
cis-18:1ω-6	5.27 ± 0.39	0.60 ± 0.06[a]	0.67 ± 0.03[a]	0.14 ± 0.02	0.063 ± 0.040	5
cis-18:1ω-9	5.49 ± 0.23	0.60 ± 0.08[a]	0.72 ± 0.08[a]	0.07 ± 0.01	0.074 ± 0.032	4
trans-18:1ω-9	5.20 ± 0.44	0.80 ± 0.08	0.89 ± 0.10	0.09 ± 0.03	0.040 ± 0.020	6
cis-18:1ω-11	4.70 ± 0.35	0.80 ± 0.12	0.94 ± 0.14	0.10 ± 0.02	0.036 ± 0.019	6
cis-18:1ω-13	5.34 ± 0.45	0.89 ± 0.03	1.07 ± 0.06	0.13 ± 0.04	0.060 ± 0.021	5

[a] Statistically significant differences with respect to the control condition ($p < 0.003$).

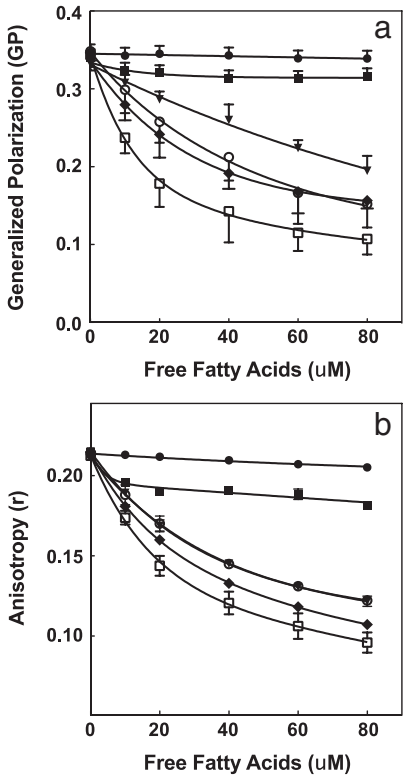

Fig. 4. Laurdan excitation GP (a) and anisotropy of the fluorescence probe DPH (b), in the presence of increasing concentrations of *cis*-18:1ω-6 (○), *cis*-18:1ω-9 (□), *cis*-18:1ω-11 (♦), *cis*-18:1ω-13 (▼) and *trans*-18:1ω-9 (■), or only vehicle (control condition, ●). Each point corresponds to the average ± S.D. of more than four independent experiments. Statistically significant differences ($p<0.01$) were found in all the experimental conditions when compared with the initial condition.

indicating that they hardly modified membrane polarity. On the other hand, all the *cis*-monounsaturated FFAs tested caused membrane order perturbations dependent on the position of the double bond (Fig. 4a), with *cis*-18:1ω-9 (oleic acid) increasing membrane fluidity the most. Because Laurdan is superficially located in the membrane, it was expected that *cis*-18:1ω-6 would be the FFA having the greatest effect on the membrane. However, this FFA, together with *cis*-18:1ω-13, perturbed GP values the least. *cis*-18:1ω-11 had an intermediate effect.

It is also possible that on account of Laurdan's shallow location in the membrane bilayer, the probe is not able to sense the actual magnitude of the perturbation caused by FFAs with their double bond in position 11 or 13. We therefore resorted to the fluorescence probe DPH that localizes deeply in the hydrophobic core of the lipid bilayer [43]. DPH has most frequently been used for studies on the structure and dynamic properties of membranes and to assess membrane fluidity and/or order [44–49]. Analogous studies were performed measuring its anisotropy. As in the case of the results obtained with Laurdan, DPH anisotropy decreased most with *cis*-18:1ω-9, followed by *cis*-18:1ω-11. *trans*-18:1ω-9 induced small and constant diminutions in DPH anisotropy (Fig. 4b). When the membranes were treated with *cis*-18:1ω-6 the DPH anisotropy perturbations differed from those in the GP studies, probably because the DPH was too distant from the double bond of *cis*-18:1ω-6 to sense its effect in the neighboring lipids. As DPH is deep inside the membrane the largest anisotropy decrease was expected to occur with FFAs having their double bond in the position furthest along the acyl chain (*cis*-18:1ω-13), but in fact the measured anisotropy values were similar to those measured with *cis*-18:1ω-6. Taking together GP and anisotropy membrane perturbations by these *cis*-monounsaturated FFAs, it is clear that the latter modify membrane order to a greater or lesser degree, depending on the location of the double bond, the highest effect being observed when the double bond is near the middle of the acyl chain. In contrast, *trans*-unsaturated FFAs had next to no effect.

3.4. FFAs induce AChR conformational changes

The AChR is an allosteric protein, which has two closed stable states: one in the absence of agonist (R) and the other induced by ~~a~~ prolonged exposure to agonists (D). Both R and D states are characterized by a distinct protein conformation [9]. In previous studies we used the value of the dissociation constant (K_D) of the AChR ion-channel blocker CrV to infer the conformational state of the AChR [14] based on the fact that CrV displays higher affinity for the D state of the AChR than for its R state [50]. We also demonstrated that both steroids and certain FFAs induced perturbations of the AChR conformational states [14]. Here, we studied the effect produced by monounsaturated FFAs on the conformational state of the AChR, using *T. californica* AChR-rich membranes with the AChR either in the R or in the D state. AChR-rich membranes were first incubated with different concentrations of FFAs (up to 80 μM) and then titrated with CrV. Fig. 5 shows the curves obtained with the normalized CrV fluorescence emission as a function of the molar concentration of CrV for the AChR in the R and D states, respectively. The latter is displaced to the left because of the higher affinity of CrV for the D state. When the membranes were previously exposed to FFAs, the experimental curves were qualitatively different for almost all the FFAs tested. In the presence of *cis*-18:1 ω-6, the curves obtained in the absence of agonist were quite similar to the control one, whereas in the presence of agonist the curves were displaced to the right, in a FFA concentration-dependent manner, approaching the control curve in the R state (Fig. 5a). When the FFA added was *cis*-18:1 ω-9, the curves obtained in the absence of agonist were displaced to the left, towards those obtained with the AChR in the D state, and in the presence of agonist they were displaced to the right, towards those obtained with the AChR in the R state: in both cases, higher FFA concentrations made for larger displacements (Fig. 5b). Fig. 6 shows the K_D values obtained with membranes treated with different monounsaturated-FFAs in the presence or absence of Carb. All unsaturated FFAs increased K_D values when the membranes were incubated in the presence of agonist (D state in the control condition).

To obtain complementary evidence on AChR conformational changes caused by FFAs, we performed quenching experiments with AChR purified from *T. californica* membranes labeled with a fluorescent lipophilic probe (pyrene-maleimide) specific for sulfhydryl groups in a hydrophobic environment following the protocol used by Narayanaswami et al. [28]. The pyrene attached to the AChR was located in a shallow position, close to the membrane-water interface

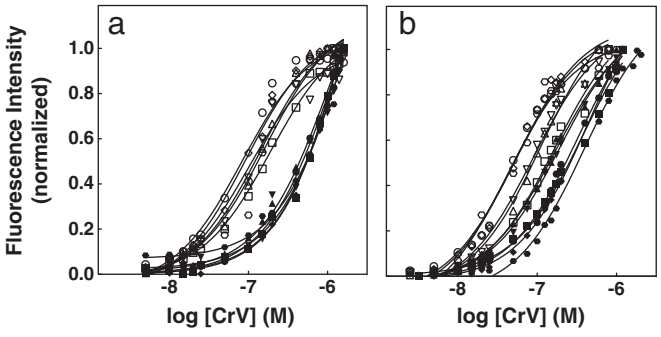

Fig. 5. Titration of AChR-rich membranes with CrV. Membranes were previously incubated for 45 min with increasing concentrations of a) *cis*-18:1ω-6 and b) *cis*-18:1ω-9 (control, ●; 10 μM, ●; 20 μM, ♦; 40 μM, ▼; 60 μM, ▲; 80 μM ■), in the absence or presence of 1 mM Carb (closed and open symbols, respectively).

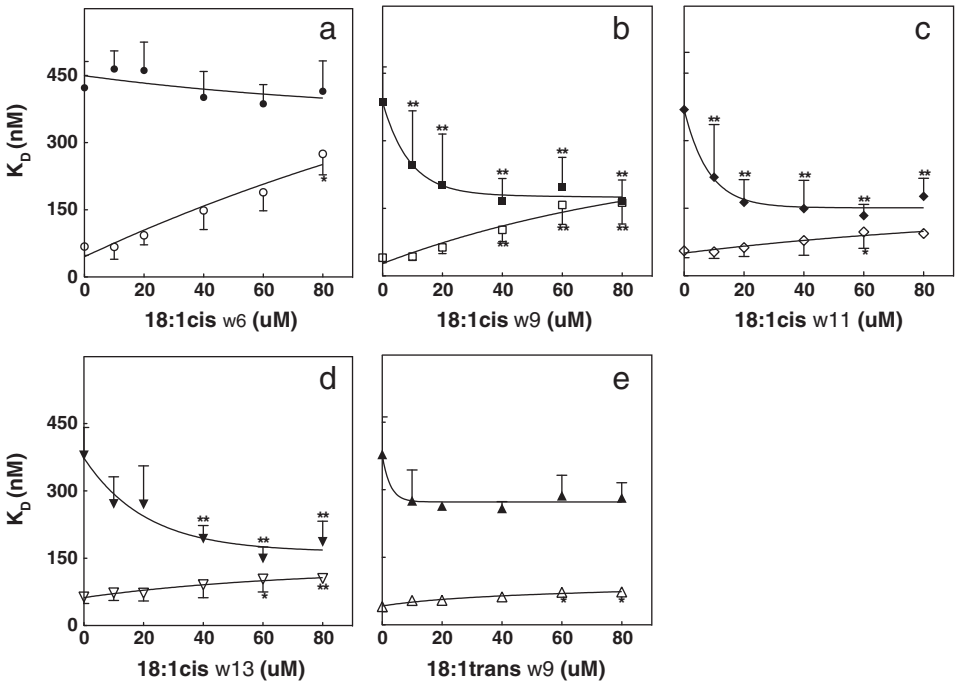

Fig. 6. Changes in K_D values of CrV by the addition of FFA. K_D values of CrV, calculated from the titration curves, as a function of increasing concentrations of a) *cis*-18:1ω-6 (●), b) *cis*-18:1ω-9 (■), c) *cis*-18:1ω-11 (♦), d) *cis*-18:1ω-13 (▼) and e) *trans*-18:1ω-9 (▲), in the absence and presence of 1 mM Carb (closed and open symbols, respectively). Each point corresponds to the average ± S.D. of more than four independent experiments. Statistically significant differences (*, $p<0.05$ and **, $p<0.01$) compared with the control values (absence of FFAs).

[28]. Spin-labeled stearic acid with the nitroxide group attached to carbon 5 (5-SLFA) was added to membranes previously treated with different FFAs. The quenching profile of the pyrene fluorescence in each case and the calculated Stern–Volmer quenching constants (K_{SV}) are shown in Figs. 7a and b, respectively. When the membrane was pre-incubated with *cis*-monounsaturated FFAs the quenching of pyrene diminished, as reflected in a decrease in K_{SV} values; cis-18:1 ω-6 exerted the lowest effect and the *trans*-monounsaturated FFA had no effect. Thus, the presence of *cis*-monounsaturated FFAs in the membrane caused a rearrangement of the pyrene position inside the membrane, implying a local topological change in the AChR γTM segment.

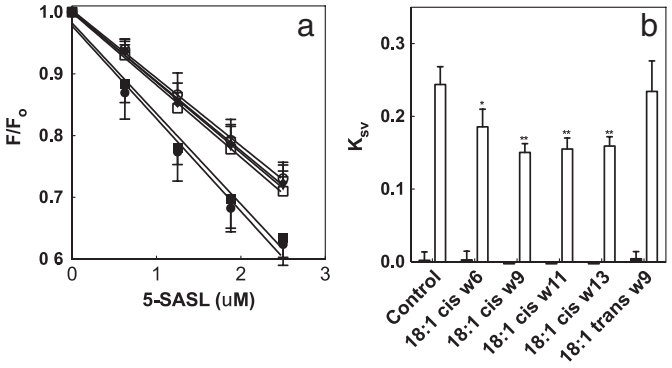

Fig. 7. Fluorescence quenching with a spin-label FFA. a) Plots of F/Fo of membranes previously treated with only vehicle (control condition, ●) or with 60 μM of *cis*-18:1ω-6 (○), *cis*-18:1ω-9 (□), *cis*-18:1ω-11 (♦), *cis*-18:1ω-13 (▼) and *trans*-18:1ω-9 (■) followed by incubation with increasing amounts of 5-SLFA. b) Stern–Volmer constants (K_{sv}) obtained from Stern–Volmer plots (Fo/F) of the data of (a). Filled and open bars correspond to K_{sv} obtained from samples treated with the vehicle for the 5-SLFA (ethanol) or with 5-SLFA, respectively. Each point/bar corresponds to the average ± S.D. of more than four independent experiments. Statistically significant differences (*, $p<0.05$ and **, $p<0.01$) compared with the control values (i.e. in the absence of FFAs).

4. Discussion

In the present study we focused on the mechanism of FFA inhibition of AChR function. Previous studies have shown that highly hydrophobic molecules such as FFAs and steroids can act as NCA of the AChR [16,51–53]. It has been proposed that FFAs may act on AChR through the protein–lipid interface, by previously partitioning inside the membrane [13,14,39,53]. Using the patch-clamp technique we have shown that irrespective of their chemical structure, four different FFAs (the unsaturated FFAs arachidonic and docosahexanoic acid and the saturated FFAs palmitic and nonadecanoic acid) inhibit AChR function. However, their mechanism of action is still not fully understood.

To learn more about the way in which FFAs affect AChR function, in the present study we focused on FFAs with a single double bond located at different positions along an 18-carbon acyl chain: petroselenic acid (*cis*-18:1ω-6), oleic acid (*cis*-18:1ω-9), vaccenic acid (*cis*-18:1ω-11), *cis*-13-octadecenoic acid (*cis*-18:1ω-13) and elaidic acid (*trans*-18:1ω-9). We used different experimental approaches to identify the main properties conditioning AChR function at the lipid–protein interface. Table 2 summarizes the results as a function of the position of the double bond of the FFA used.

Trp and Laurdan constitute a good donor–acceptor pair for FRET measurements, with a minimum donor–acceptor distance of 14 Å which roughly corresponds to the diameter of the first shell of lipids surrounding the AChR TM region [37]. Whatever moves Laurdan molecules away from the AChR environment will decrease FRET efficiency, as is the case with exogenous hydrophobic molecules [37]. However, depending on the location of these exogenous compounds at the lipid-AChR interface, i.e. annular and/or non-annular sites, the profile of the diminution varies. All the FFAs studied partitioned at the lipid-AChR microenvironment; all, except *cis*-18:1ω-6, located at both annular and non-annular sites (Fig. 2). It is noteworthy that only *cis*-18:1ω-6, whose double bond is located more superficially inside the membrane, was restricted to annular sites.

Once confirmed that all FFAs partitioned at the lipid-AChR interface, functional studies were performed using the patch-clamp

Table 2
Summary of the experimental data obtained with different FFAs.

	cis-18:1ω6	*cis*-18:1ω9	*cis*-18:1ω11	*cis*-18:1ω13	*trans*-18:1ω9
Sites at lipid-AChR interface	A[a]	A + NA[b]	A + NA	A + NA	A + NA
AChR function inhibition	+	++	–	–	–
GP modification	++	+++	++	+	–
Anisotropy modification	+	+++	++	++	–
R-state perturbation	–	++	++	++	–
M4 perturbation	+	++	++	++	–
D-state perturbation	++	++	+	+	+

[a]A: annular sites, [b]NA: non-annular sites.

technique. Unexpectedly, not just any monounsaturated FFA alters the muscle type AChR in the same manner: only *cis*-18:1ω-6 and *cis*-18:1ω-9 could alter single channel currents. The net effect of these two FFAs was a diminution in both the mean open time duration and the mean burst duration (Table 1). The latter modification is in agreement with a shortening of the main open component duration, reflecting, as previously stated, single apertures. The site of action of these two FFAs seems to be distant from the channel pore since no flickering behavior was observed in the single-channel recordings. Moreover, since none of the other kinetic parameters were modified after pre-incubation with both FFAs, we can infer that the receptor undergoes a transition from the inhibited state to its closed conformation. The other two monounsaturated FFAs tested, *cis*-18:1ω-11 and *cis*-18:1ω-13, exerted no effect on AChR function. The key difference between the different FFAs studied here resides in the double bond: *cis*-18:1ω-6 and *cis*-18:1ω-9, which effectively behaved as AChR inhibitors, have the double bond at a more superficial location, whereas *cis*-18:1ω-11 and *cis*-18:1ω-13, the two *cis*-FFAs with no inhibitory effect, have the double bond more deeply inside the membrane. Interestingly, *trans*-18:1ω-9, with the double bond at the same position as *cis*-18:1ω-9 but with an isomerism which leads to a different spatial arrangement, did not modify channel kinetics. Previous studies also demonstrated that other FFAs with different chemical structures (18:0, 20:0, 18:2, 18:3, 20:4 and 22:6) localize at annular and non-annular sites [14,19], and that 20:0, 20:4 and 22:6 act as AChR inhibitors [54]. Taking together the fact that not all FFAs inhibit AChR function and that all FFAs localize at the lipid-AChR interface but not all at the same boundary sites, the location in non-annular sites may not be a prerequisite for AChR inhibition.

To determine whether inhibition of AChR function –or the lack of it– by certain FFAs can be explained by the biophysical characteristics of the AChR-lipid environment, we studied the effect of each FFA on the biophysical properties of AChR-rich membranes. GP of the fluorescence probe Laurdan and anisotropy experiments with DPH shows that all *cis*-monounsaturated FFAs modify membrane order, albeit to different extents, depending on their chemical structure. Oleic acid (*cis*-18:1ω-9) affects this property more than all other FFAs, a perturbation that can be related to the fact that this FFA exerts the strongest inhibitory effect on the AChR. Petroselenic acid (*cis*-18:1ω-6) has the same effect as that of vaccenic acid (*cis*-18:1ω-11) according to GP and to *cis*-13-octadecenoic acid (*cis*-18:1ω-13) anisotropy studies. Since these latter two FFAs did not inhibit the AChR but did modify the membrane order in the same manner as *cis*-18:1ω-6, we conclude that changes in membrane fluidity as a consequence of the addition of FFAs are not per se responsible for AChR inhibition.

Complementary studies of AChR conformational changes in the presence of FFAs were performed with the fluorescence dye CrV which displays different affinities for the R and D states of the AChR. Desensitizing concentration of agonist decreased the K_D for CrV, indicating that AChR undergoes conformational changes leading to the high-affinity D state [55]. When AChR-rich membranes in the R-state were incubated with the *cis*-monounsaturated FFAs, all except *cis*-18:1 ω-6 decreased K_D to values approaching those observed for the agonist-induced D state. This result indicates that certain FFAs induce a conformational change in the AChR, suggesting a direct correlation between localization at non-annular sites and perturbation of the AChR R-state. However, these conformational changes do not suffice to account for the inhibitory effect of FFAs on AChR, since in the R-state *cis*-18:1ω-9 produced a conformational change whereas *cis*-18:1ω-6 did not. *trans*-18:1ω-9 caused no modification of K_D values although it localizes at both annular and non-annular sites, suggesting that it is the kink of the double bond that is responsible for AChR R-state perturbations. When similar studies were performed in the presence of agonist, all monounsaturated FFAs modified the D state of AChR by increasing the K_D values. However, a marked differentiation in the profile of variation between *cis*-18:1ω-6 and ω-9 on the one hand and the rest of the FFAs on the other, can be appreciated. Higher perturbations of the AChR D-state, which can be related to *cis*-monounsaturated FFAs with the double bond at positions relatively superficial at the lipid–protein interface, independently of the sites they occupy, can be correlated with AChR-inhibition.

An additional experiment focusing on AChR conformation was carried out: the topological position of the M4 TM segments, which has extensive contact with the lipid bilayer [3], was then evaluated in the presence of the monounsaturated FFAs. Although M4 is relatively far from both the channel lumen and the transmitter binding sites, functional analyses have shown that mutations of some of the residues in the M4 segment of different AChR subunits alter the gating equilibrium constant [56–60]. These and other results suggest that M4 residues experience a synchronous motion during the gating reaction [55–59]. Fluorescence quenching experiments with purified AChR from *Torpedo* membrane labeled with N-PyrM in the presence of FFAs showed that the presence of all *cis*-monounsaturated FFAs led to a conformational change in the TM portion of the AChR. Two groups of compounds can be proposed based on the different statistical significance level of *cis*-18:1ω-6 ($p<0.05$) compared with the rest of the *cis*-unsaturated FFAs ($p<0.01$). These can be related to different site locations at the lipid-AChR interface: higher significance levels could correspond to M4 topological perturbations at both annular and non-annular sites, whereas lower M4 topological perturbations could indicate the presence of FFAs only at annular sites. The fact that the presence of *trans*-18:1ω-9 inside the membrane did not modify K_{sv} even though it localizes at both annular and non-annular sites further supports this interpretation: the kink of the double bond may be responsible for the occurrence of M4 topological perturbations, whereas their magnitude is likely related to the localization of the FFAs. As stated above, AChR conformational perturbations as a consequence of localization at different sites are not sufficient to fully explain the inhibitory effect of FFAs on AChR function.

Clearly, FFAs exert different effects on the AChR conformational state depending on their structural characteristics: the presence, position and isomerism of the double bond seem to play an important role in the modification of the conformational state of the AChR both in its R and D states. There is a correlation between the localization of certain molecules at non-annular sites and perturbation of the AChR R state without necessarily affecting AChR function, whereas perturbations of the AChR D-state by the presence of molecules at annular and/or non-annular sites can be related to the AChR inhibition

function. Taken together, these data lead us to conclude that the position of the torsion angle of unsaturated FFAs is a key factor in channel blockage.

The sequence of structural events coupling ligand binding with channel gating is considered a conserved core mechanism: it is postulated to begin with movements at the ligand-binding loops, followed by the displacement of loops located at the interface between the extracellular ligand binding domain and the TM domain, continuing with the tilting/bending of the pore-lining M2 helix, and ending with movements of M4, M3 and M1 helices in the TM domain [61,62]. FFAs exert their action by an allosteric mechanism at the lipid-AChR interface: all FFAs effectively localize in the environment of the protein, not all at the same sites, and they are all detected by the AChR as indicated by the changes in the topology of the M4 segment in their presence. However, only those FFAs having the double bond at a superficial position relative to the lipid bilayer were found to act as AChR inhibitors. This suggests that those FFAs with the double bond at a superficial position inside the membrane are probably at the level of the conserved core structure for AChR gating and hence could perturb this synchronous mechanism.

Acknowledgements

This work was supported in part by grants from the *Agencia Nacional de Promoción Científica* (FONCYT) to F.J.B., and from the *Universidad Nacional del Sur* and the *Consejo Nacional de Investigaciones Científicas y Técnicas* to F.J.B. and S.S.A.

References

[1] S.L. Hamilton, D.R. Pratt, D.C. Eaton, Arrangement of the subunits of the nicotinic acetylcholine receptor of *Torpedo californica* as determined by alpha-neurotoxin crosslinking, Biochemistry 24 (1985) 2210–2219.
[2] A. Karlin, Ion channel structure emerging structure of the nicotinic acetylcholine receptors, Nat. Rev. Neurosci. 3 (2002) 102–114.
[3] F.J. Barrantes, Modulation of nicotinic acetylcholine receptor function through the outer and middle rings of transmembrane domains, Curr. Opin. Drug Discov. Dev. 6 (2003) 620–632.
[4] F.J. Barrantes, Structural basis for lipid modulation of nicotinic acetylcholine receptor function, Brain Res. Rev. 47 (2004) 71–95.
[5] D. Marsh, F.J. Barrantes, Immobilized lipid in acetylcholine receptor-rich membranes from *Torpedo marmorata*, Proc. Natl. Acad. Sci. U. S. A. 75 (1978) 4329–4333.
[6] D. Marsh, A. Watts, F.J. Barrantes, Phospholipid chain immobilization and steroid rotational immobilization in acetylcholine receptor-rich membranes from *Torpedo marmorata*, Biochim. Biophys. Acta 645 (1981) 97–101.
[7] S.B. Mantipragada, L.I. Horváth, H.R. Arias, G. Schwarzmann, K. Sandhoff, F.J. Barrantes, D. Marsh, Lipid–protein interactions and effect of local anesthetics in acetylcholine receptor-rich membranes from *Torpedo marmorata* electric organ, Biochemistry 42 (2003) 9167–9175.
[8] I.E. Andreeva, S. Nirthanan, J.B. Cohen, S.E. Pedersen, Site specificity of agonist-induced opening and desensitization of the *Torpedo californica* nicotinic acetylcholine receptor, Biochemistry 45 (2006) 195–204.
[9] A.L. Auerbach, G. Akk, Desensitization of mouse nicotinic acetylcholine receptor channels, J. Gen. Physiol. 112 (1998) 181–197.
[10] S.J. Edelstein, O. Schaad, E. Henry, D. Bertrand, J.P. Changeux, A kinetic mechanism for nicotinic acetylcholine receptors based on multiple allosteric transitions, Biol. Cybern. 75 (1996) 361–379.
[11] S.E. Ryan, C.N. Demers, J.P. Chew, J.E. Baenziger, Structural effects of neutral and anionic lipids on the nicotinic acetylcholine receptor, J. Biol. Chem. 271 (1996) 24590–25497.
[12] Y. Xu, F.J. Barrantes, X. Luo, K. Chen, J. Shen, H. Jiang, Conformational dynamics of the nicotinic acetylcholine receptor channel: a 35-ns molecular dynamics simulation study, J. Am. Chem. Soc. 127 (2005) 1291–1299.
[13] G.A. Fernández Nievas, F.J. Barrantes, S.S. Antollini, Conformation-sensitive steroid and fatty acid sites in the transmembrane domain of the nicotinic acetylcholine receptor, Biochemistry 46 (2007) 3503–3512.
[14] G.A. Fernández Nievas, F.J. Barrantes, S.S. Antollini, Modulation of nicotinic acetylcholine receptor conformational state by free fatty acids and steroids, J. Biol. Chem. 283 (2008) 21478–21486.
[15] C.J.B. daCosta, J.E. Baenziger, A lipid-dependent uncoupled conformation of the acetylcholine receptor, J. Biol. Chem. 284 (2009) 17819–17825.
[16] S. Minota, S. Watanabe, Inhibitory effects of arachidonic acid on nicotinic transmission in bullfrog sympathetic neurons, J. Neurophysiol. 78 (1997) 2396–2401.
[17] J.E. Baenziger, M.L. Morris, T.E. Darsaut, S.E. Ryan, Effect of membrane lipid composition on the conformational equilibria of the nicotinic acetylcholine receptor, J. Biol. Chem. 275 (2000) 777–784.
[18] O.T. Jones, M.G. McNamee, Annular and nonannular binding sites for cholesterol associated with the nicotinic acetylcholine receptor, Biochemistry 27 (1988) 2364–2374.
[19] S.S. Antollini, F.J. Barrantes, Disclosure of discrete sites for phospholipid and sterols at the protein–lipid interface in native acetylcholine receptor-rich membrane, Biochemistry 37 (1998) 16653–16662.
[20] F.J. Barrantes, Interactions between the acetylcholine receptor and the non-receptor, peripheral nu peptide (Mr 43000), in: F. Hucho (Ed.), Neuroreceptors, W. de Gruyter, Berlin, New York, 1982, pp. 315–328.
[21] P.R. Hartig, M.A. Raftery, Preparation of right-side-out, acetylcholine receptor enriched intact vesicles from *Torpedo californica* electroplaque membranes, Biochemistry 18 (1979) 1146–1150.
[22] C. Gutiérrez-Merino, I.C. Bonini de Romanelli, L.I. Pietrasanta, F.J. Barrantes, Preferential distribution of the fluorescent phospholipid probes NBD-phosphatidylcholine and rhodamine-phosphatidylethanolamine in the exofacial leaflet of acetylcholine receptor-rich membranes from *Torpedo marmorata*, Biochemistry 34 (1995) 4846–4855.
[23] C.J.B. daCosta, A.A. Ogrel, E.A. McCardy, M.P. Blanton, J.E. Baenziger, Lipid–protein interactions at the nicotinic acetylcholine receptor: a unique coupling between nicotinic receptors and phosphatidic acid containing lipid bilayers, J. Biol. Chem. 277 (2001) 201–208.
[24] C.J.B. daCosta, I.D. Wagg, M.E. Mckay, J.E. Baenziger, Phosphatidic acid and phosphatidylserine have distinct structural and functional interactions with the nicotinic acetylcholine receptor, J. Biol. Chem. 279 (2004) 14967–14974.
[25] O.H. Lowry, N.J. Rosebrough, L.A. Farr, R.J. Randall, Protein measurement with the Folin phenol reagent, J. Biol. Chem. 193 (1951) 265–275.
[26] L. Li, M. Schuchard, A. Palma, L. Pradier, M.G. McNamee, Functional role of the cysteine 451 thiol group in the M4 helix of the γ subunit of *Torpedo californica* acetylcholine receptor, Biochemistry 29 (1990) 5428–5436.
[27] V. Narayanaswami, J. Kim, M.G. McNamee, Protein–lipid interactions and *Torpedo californica* nicotinic acetylcholine receptor function. 1. Spatial disposition of cysteine residues in the gamma subunit analyzed by fluorescence-quenching and energy-transfer measurements, Biochemistry 32 (1993) 12413–12419.
[28] V. Narayanaswami, M.G. McNamee, Protein–lipid interactions and *Torpedo californica* nicotinic acetylcholine receptor function. 2. Membrane fluidity and ligand-mediated alteration in the accessibility of γ subunit cysteine residues to cholesterol, Biochemistry 32 (1993) 12420–12427.
[29] A.M. Roccamo, M.F. Pediconi, E. Aztiria, L. Zanello, A. Wolstenholme, F.J. Barrantes, Cells defective in sphingolipids biosynthesis express low amounts of muscle nicotinic acetylcholine receptor, Eur. J. Neurosci. 11 (1999) 1615–1623.
[30] O.P. Hamill, A. Marty, E. Neher, B. Sakmann, F.J. Sigworth, Improved patch-clamp techniques for high-resolution current recording from cells and cell-free membrane patches, Pflügers Arch. Eur. J. Physiol. 391 (1981) 85–100.
[31] T. Parasassi, G. De Stasio, A. d'Ubaldo, E. Gratton, Phase fluctuation in phospholipid membranes revealed by Laurdan fluorescence, Biophys. J. 57 (1990) 1179–1186.
[32] T. Parasassi, G. De Stasio, G. Ravagnan, R.M. Rusch, E. Gratton, Quantitation of lipid phases in phospholipid vesicles by the generalized polarization of Laurdan fluorescence, Biophys. J. 60 (1991) 179–189.
[33] M. Shinitzky, Y. Yuli, Lipid fluidity at the submacroscopic level: determination by fluorescence polarization, Chem. Phys. Lipids 30 (1982) 261–282.
[34] J. Lakowicz, Principles of Fluorescence Spectroscopy, Second Edition Plenum Publishers, New York, 1999.
[35] T. Förster, Intermolecular energy transference and fluorescence, Ann. Phys. 2 (1948) 55–75.
[36] M. Vincent, L.S. England, J.T. Trevors, Cytoplasmic membrane polarization in Gram-positive and Gram-negative bacteria grown in the absence and presence of tetracycline, Biochim. Biophys. Acta 1672 (2004) 131–134.
[37] S.S. Antollini, M.A. Soto, I. Bonini de Romanelli, P. Sotomayor, F.J. Barrantes, Physical state of bulk and protein-associated lipid in nicotinic acetylcholine receptor-rich membrane studied by laurdan generalized polarization and fluorescence energy transfer, Biophys. J. 70 (1996) 1275–1284.
[38] A.G. Lee, How lipids affect the activities of integral membrane proteins, Biochim. Biophys. Acta 1666 (2004) 62–87.
[39] C. Bouzat, F.J. Barrantes, Effects of long-chain fatty acids on the channel activity of the nicotinic acetylcholine receptor, Receptors Channels 1 (1993) 251–258.
[40] S.M. Sine, J.H. Steinbacht, Activation of acetylcholine receptors on clonal mammalian BC3H-1 cells by low concentrations of agonist, J. Physiol. 373 (1986) 129–162.
[41] W. Yu, P.T.C. So, T. French, E. Gratton, Fluorescence generalized polarization of cell membranes: a two-photon scanning microscopy approach, Biophys. J. 70 (1996) 626–636.
[42] F.M. Harris, K.B. Best, J.D. Bell, Use of laurdan fluorescence intensity and polarization to distinguish between changes in membrane fluidity and phospholipid order, Biochim. Biophys. Acta 1565 (2002) 123–128.
[43] R. Kaiser, E. London, Location of diphenylhexatriene (DPH) and its derivatives within membranes: comparison of different fluorescence quenching analyses of membrane depth, Biochemistry 37 (1998) 8180–8190.
[44] B.R. Lentz, S.W. Burgess, A dimerization model for the concentration dependent photophysical properties of diphenylhexatriene and its phospholipid derivatives DPHpPC and DPHpPA, Biophys. J. 56 (1989) 723–733.
[45] G. Zolese, E. Gratton, G. Curatola, Phosphatidic acid affects structural organization of phosphatidylcholine liposomes. A study of 1,6-diphenyl-1,3,5-hexatriene (DPH) and 1-(4-trimethylammonium-phenyl)-6-phenyl,1,3,5-hexatriene (TMA-DPH) fluorescence decay using distributional analysis, Chem. Phys. Lipids 55 (1990) 29–39.
[46] B.R. Lentz, J.R. Wu, L. Zheng, J. Prevrátil, The interfacial region of dipalmitoylphosphatidylcholine bilayers is perturbed by fusogenic amphipaths, Biophys. J. 71 (1996) 3302–3310.

[47] C.A. Valcarcel, M. Dalla Serra, C. Potrich, I. Bernhart, M. Tejuca, D. Martinez, F. Pazos, M.E. Lanio, G. Menestrina, Effects of lipid composition on membrane permeabilization by sticholysin I and II, two cytolysins of the sea anemone *Stichodactyla helianthus*, Biophys. J. 80 (2001) 2761–2774.
[48] C. Nunes, C. Sousa, H. Ferreira, M. Lucio, J.L.F.C. Lima, J. Tavares, A. Cordeiro da Silva, S. Reis, Effect of nonsteroidal anti-inflammatory drugs on the cellular membrane fluidity, J. Environ. Biol. 29 (2008) 733–738.
[49] K. Reiss, I. Cornelsen, M. Husmann, G. Gimpl, S. Bhakdi, Unsaturated fatty acids drive ADAM-dependent cell adhesion, proliferation and migration by modulating membrane fluidity, J. Biol. Chem. 286 (2011) 26931–26942.
[50] M.M. Lurtz, S.E. Pedersen, Aminotriarylmethane dyes are high-affinity noncompetitive antagonists of the nicotinic acetylcholine receptor, Mol. Pharmacol. 55 (1999) 159–167.
[51] T.J. Andreasen, M.G. McNamee, Inhibition of ion permeability control properties of acetylcholine receptor from *Torpedo californica* by long-chain fatty acids, Biochemistry 19 (1980) 4719–4726.
[52] C. Bouzat, F.J. Barrantes, Hydrocortisone and 11-desoxycortisone modify acetylcholine receptor channel gating, Neuroreport 4 (1993) 143–146.
[53] M.P. Blanton, Y. Xie, L.J. Dangott, J.B. Cohen, The steroid promegestone is a noncompetitive antagonist of the *Torpedo* nicotinic acetylcholine receptor that interacts with the lipid–protein interface, Mol. Pharmacol. 55 (1999) 269–278.
[54] S.S. Antollini, F.J. Barrantes, Unique effects of different fatty acid species on the physical properties of the *Torpedo* acetylcholine receptor membrane, J. Biol. Chem. 277 (2002) 1249–1254.
[55] C.B. Bouzat, H. Lacorazza, M. Biscoglio de Jiménez Bonino, F.J. Barrantes, Effect of chemical modification of extracellular histidyl residues on the channel properties of the nicotinic acetylcholine receptor, Pflügers Arch. Eur. J. Physiol. 423 (1993) 365–371.
[56] I. Garbus, C. Bouzat, F.J. Barrantes, Steroids differentially inhibit the nicotinic acetylcholine receptor, Neuroreport 12 (2001) 227–231.
[57] S.I. Ortiz Miranda, J.A. Lasalde, P.A. Pappone, M.G. McNamee, Mutations in the M4 domain of the *Torpedo californica* nicotinic acetylcholine receptor alter channel opening and closing, J. Membr. Biol. 158 (1997) 17–30.
[58] S. Tamamizu, Y.H. Lee, B. Hung, M.G. McNamee, J.A. Lasalde-Dominicci, Alteration in ion channel function of mouse nicotinic acetylcholine receptor by mutations in the M4 transmembrane domain, J. Membr. Biol. 170 (1999) 157–164.
[59] C. Bouzat, F.J. Barrantes, S.M. Sine, Hydrogen bonding by conserved threonine contributes to channel gating kinetics, J. Gen. Physiol. 115 (2000) 663–672.
[60] Y.H. Lee, L. Li, J. Lasalde, L. Rojas, M.G. McNamee, S.I. Ortiz Miranda, P. Pappone, Mutations in the M4 domain of *Torpedo californica* acetylcholine receptor dramatically alter ion channel function, Biophys. J. 66 (1994) 646–653.
[61] A. Mitra, T.D. Bailey, A.L. Auerbach, Structural dynamics of the M4 transmembrane segment during acetylcholine receptor gating, Structure 12 (2004) 1909–1918.
[62] A.L. Auerbach, Gating of acetylcholine receptor channels: Brownian motion across a broad transition state, Proc. Natl. Acad. Sci. U. S. A. 102 (2005) 1408–1412.